Supplement of Atmos. Chem. Phys., 25, 16331–16346, 2025 https://doi.org/10.5194/acp-25-16331-2025-supplement © Author(s) 2025. CC BY 4.0 License.





# Supplement of

# Measurement report: Variations and environmental impacts of atmospheric $N_2O_5$ concentrations in urban Beijing during the 2022 Winter Olympics

Tiantian Zhang et al.

Correspondence to: Weili Lin (linwl@muc.edu.cn) and Chunxiang Ye (c.ye@pku.edu.cn)

The copyright of individual parts of the supplement might differ from the article licence.

#### Sect. S1 Technical details of CRDS

1

2

12

## Sect. S1.1 Determination of the Limit of Detection (LOD)

- 3 The LOD of the CRDS analyzer for N<sub>2</sub>O<sub>5</sub> was determined via a 4-hour zero-air injection experiment: zero
- 4 air (free of target analytes) was continuously introduced into the instrument cavity (1 s time resolution), and
- 5 Allan variance analysis was applied to evaluate system stability (Figure S1). The LOD was calculated using Eq.
- 6 (S1) below, yielding a value of 2.9 pptv.

$$[A] = \frac{R_L}{c\sigma} \left( \frac{1}{\tau} - \frac{1}{\tau_0} \right) \tag{S1}$$

- 8 where [A] denotes the analyte concentration, " $R_L$ " is the tratio of the cavity length to the length over which
- 9 the absorber is present, c is the speed of light,  $\sigma$  is the absorption cross-section,  $\tau$  is the cavity ring-down time
- 10 with sample gas, and τ<sub>0</sub> is the background ring-down time with zero air. During the zero-air experiment, the
- instrument background level (τ<sub>0</sub>) was measured as 50 μs.

#### Sect. S1.2 Calibration

- To ensure measurement accuracy, we performed regular calibrations using stable, calibrated NO<sub>3</sub> and N<sub>2</sub>O<sub>5</sub>
- standard sources (generated via a dynamic standard gas system, NO<sub>3</sub> generated by the reaction of NO<sub>2</sub> and O<sub>3</sub>,
- 15 N<sub>2</sub>O<sub>5</sub> generated by the equilibrium of NO<sub>3</sub> and NO<sub>2</sub>, as referenced in our prior work: Zhang et al., 2026). These
- 16 calibrations quantified two critical correction factors addressing sampling losses
- Tubing loss: Measured at  $11.4 \pm 1.3\%$ .
- Filter membrane loss: Quantified as  $4.5 \pm 0.5\%$
- The final concentrations of  $[NO_3 + N_2O_5]$  and derived  $NO_3$  were obtained by dividing raw instrument
- 20 measurements by the sum of these loss ratios (i.e., correcting for signal reduction during sample transport).

## 21 Sect. S1.3 Uncertainty

- Parameter uncertainties in concentration calculation: The absorption cross-section (σ) and effective
- absorption cavity length—key parameters in Eq. (1)—contribute 13% and 4% uncertainty, respectively.
- Data correction uncertainties: Corrections for membrane loss  $(4.5 \pm 0.5\%)$  and pipeline loss  $(11.4 \pm 1.3\%)$
- during sample transport introduce an additional 1.4% uncertainty.

The total combined uncertainty was calculated following the method described in our prior work (Zhang et al., 2024), confirming the 13.7% value.

28

29

26

27

References:

- 30 Zhang, T., Zuo, P., Ma, J., Ye, C., Lin, W., and Zhu, T.: Characterization and Application of an Online
- 31 Measurement System for NO<sub>3</sub> and N<sub>2</sub>O<sub>5</sub> Based on Cavity Ring-Down Spectroscopy, Acta Sci. Nat. Univ. Pekin.,
- 32 60, 563–574, https://doi.org/10.13209/j.0479-8023.2024.030, 2024

Zhang, T., Ma, J., Liu, T., Lin, W., Zuo, P., and Ye, C.: A dynamic generation system for NO<sub>3</sub> and N<sub>2</sub>O<sub>5</sub> standard

34 gases, Environ. Chem., 45, 1–7, https://doi.org/10.7524/j.issn.0254-6108.2024091302, 2026.

35

33

36

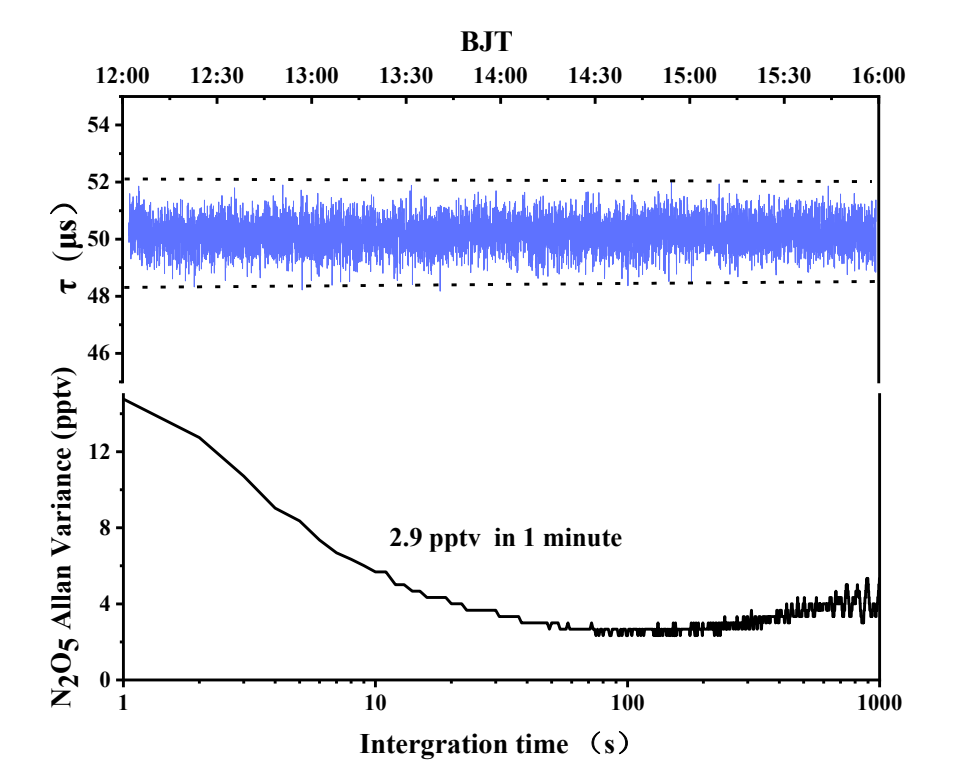
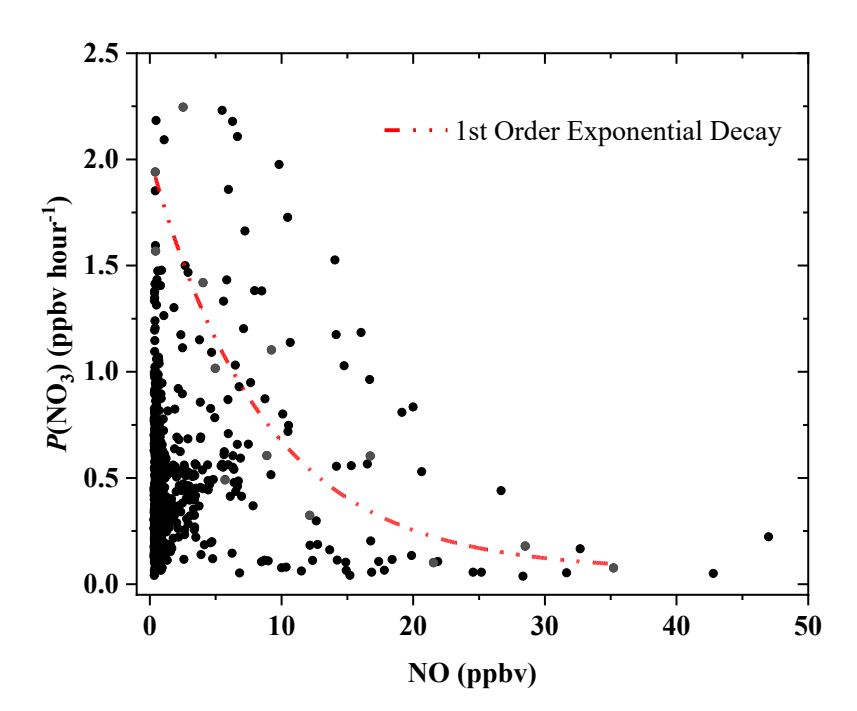


Figure S1. Limit of detection (LOD) and background signal of the instrument (blue line).



41 Figure S2. Schematic diagram of the correlation between NO and *P*(NO<sub>3</sub>).

40

42

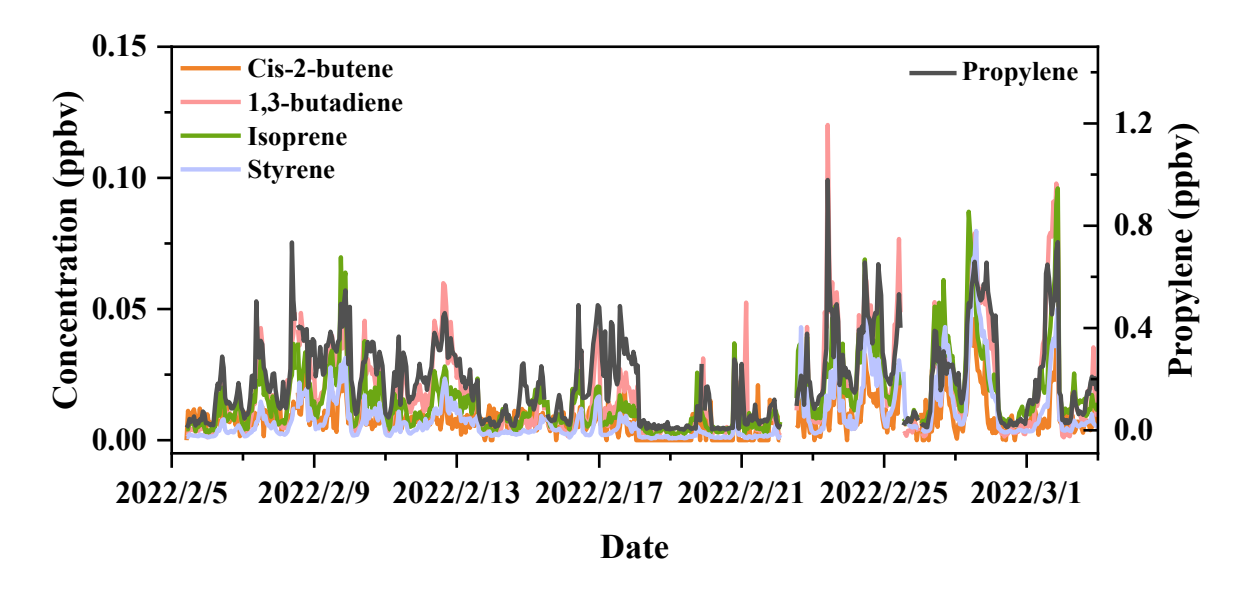
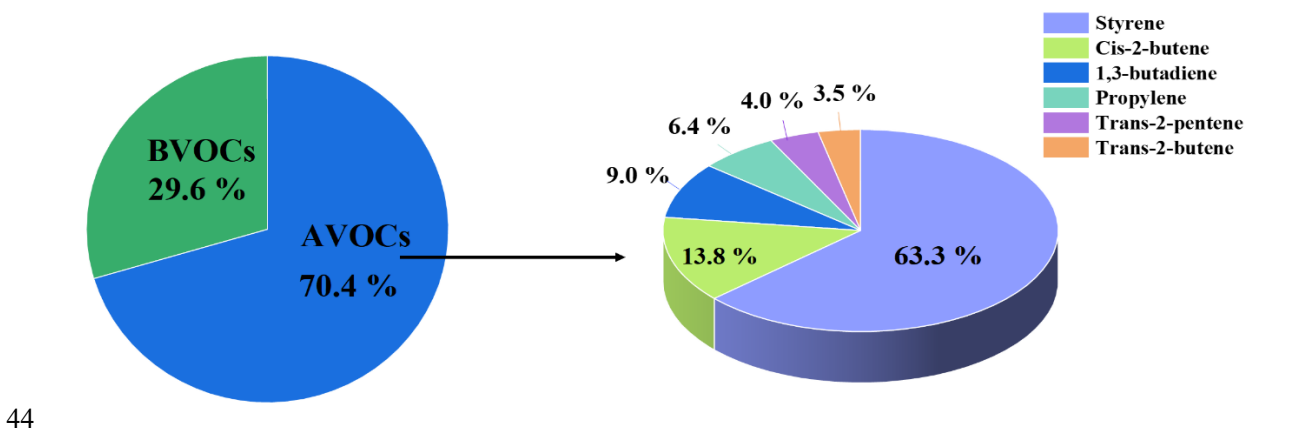
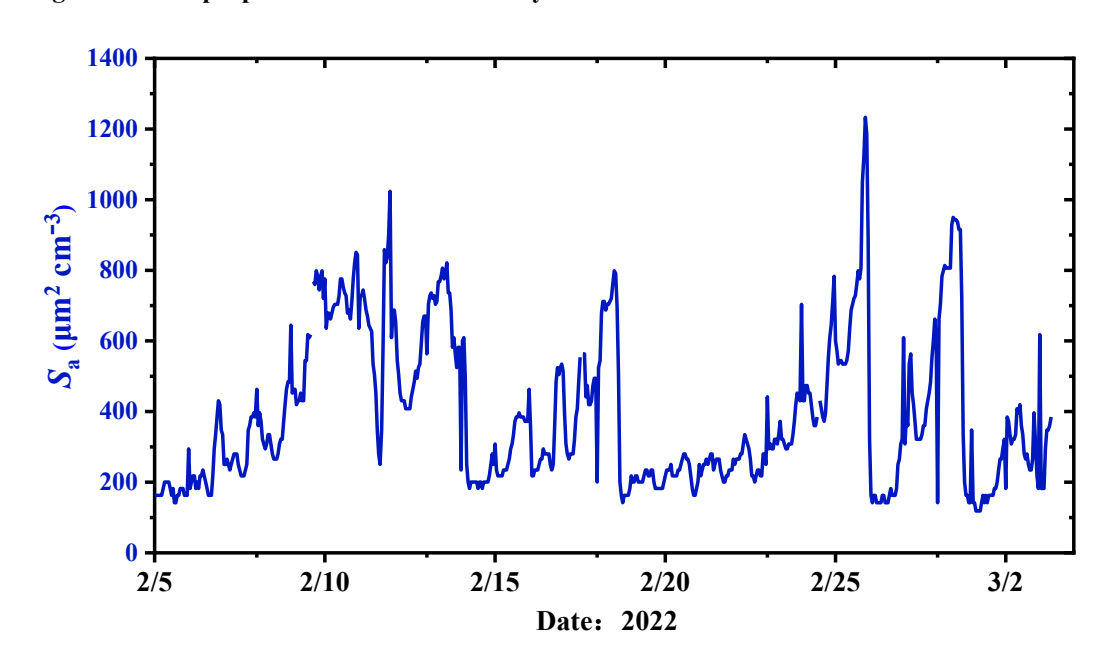


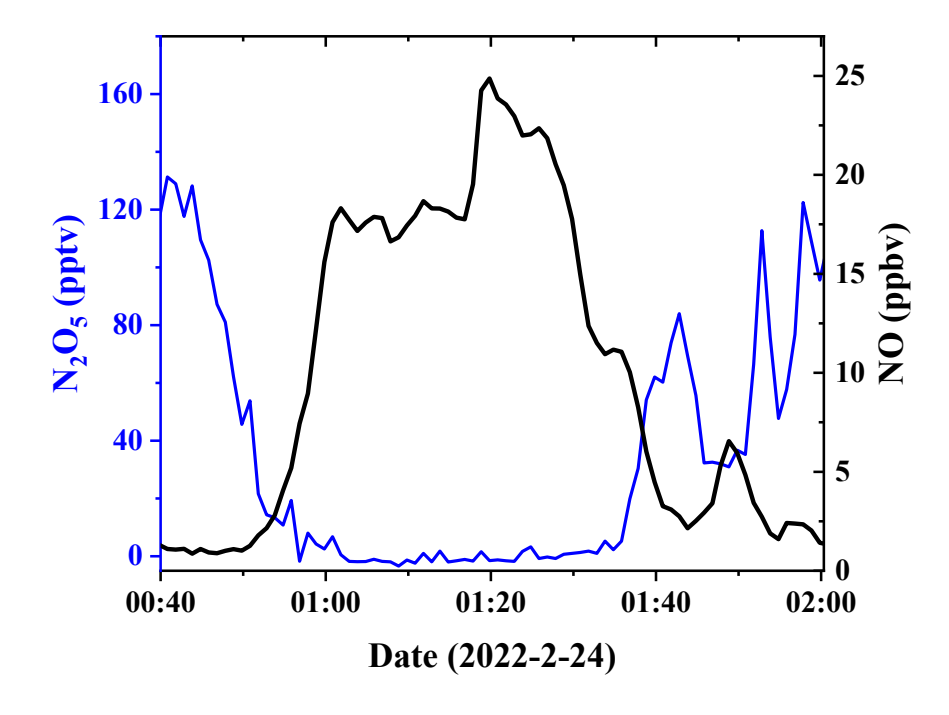
Figure S3. Temporal trends of highly reactive VOC concentrations during the observation period.



45 Figure S4. The proportion of reaction activity of NO<sub>3</sub> with different VOCs.



47 Figure S5. Time-series variations in 1h-mean  $S_a$ .



49 Figure S6. Variations in NO and N<sub>2</sub>O<sub>5</sub> mixing ratios on Feb. 24, 2022.

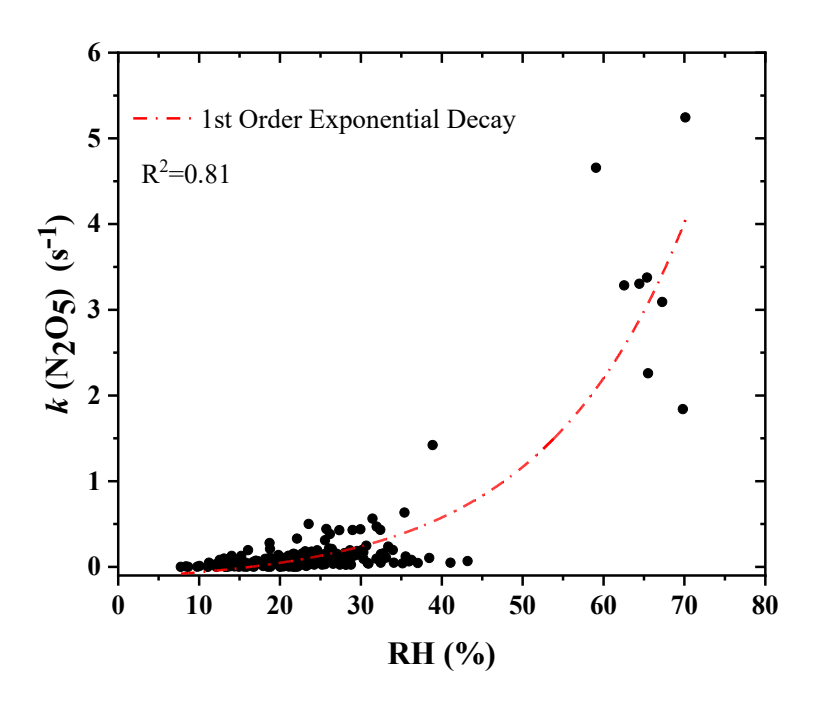


Figure S7. Schematic diagram of the correlation between RH and  $k_{\rm N_2O_5}$ .

VOCs	OGP	POP	k (298K)	
	Concentration (ppbv)	Concentration (ppbv)	(10 <sup>-15</sup> cm <sup>3</sup> molecule <sup>-1</sup> s <sup>-1</sup> )	
Ethane	3.61±1.55	4.03±2.12	0.01	
Propane	1.91±0.97	2.46±1.67	< 0.07	
Acetylene	1.41±1.04	1.61±1.09	0.21	
Acetone	1.27±0.43	1.55±0.71	< 0.03	
Ethylene	1.27±1.08	1.44±1.22	0.0049	
Styrene	$0.006 \pm 0.01$	$0.01 \pm 0.01$	1500	
Cis-2-butene	$0.007 \pm 0.01$	$0.01 \pm 0.01$	352	
1,3-butadiene	$0.02 \pm 0.01$	$0.02 \pm 0.02$	100	
Propylene	$0.18\pm0.15$	$0.22\pm0.19$	9.49	
Isoprene (BVOC)	0.01±0.01	$0.02 \pm 0.02$	696	

Table S2. N<sub>2</sub>O<sub>5</sub> uptake coefficients and NO<sub>3</sub> loss rate coefficients from a nightly steady state analysis.

Start Time-End Time	$\gamma(N_2O_5)$	k(NO <sub>3</sub> )(s <sup>-1</sup> )	Start Time-End Time	$\gamma(N_2O_5)$	k(NO <sub>3</sub> ) (s <sup>-1</sup> )
2/06 0:00 - 2/06 05:40	0.0325	0.0713	2/19 20:40 - 2/20 06:00	0.0222	0.1214
2/06 19:00 - 2/07 05:40	0.0216	0.0999	2/20 19:20 - 2/21 06:20	0.011	0.1395
2/07 19:00 - 2/08 06:40	0.0198	0.0868	2/21 20:20 - 2/22 06:00	0.0285	0.1368
2/08 19:20 - 2/09 05:20	0.0296	0.2163	2/22 19:40 - 2/23 06:40	0.0108	0.1847
2/09 18:40 - 2/10 04:00	0.0042	0.3108	2/23 19:00 - 2/24 00:20	0.0053	0.2358
2/10 19:40 - 2/11 04:40	0.0108	0.0384	2/25 19:00 - 2/26 06:40	0.0101	0.062
2/11 18:40 - 2/12 06:40	0.0155	0.0097	2/26 18:20 - 2/27 02:40	0.024	0.1655
2/13 19:00 - 2/14 07:00	0.2244	0.7001	2/27 18:40 - 2/28 20:20	0.0345	0.2158
2/14 18:40 - 2/15 06:20	0.0162	0.3441	2/28 22:00 - 3/01 06:40	0.1232	0.0111
2/15 19:20 - 2/16 05:40	0.0125	0.1554	3/01 18:20 - 3/02 03:00	0.0395	0.0887
2/16 18:20 - 2/17 06:20	0.0043	0.1996	3/02 18:40 - 3/03 04:40	0.0014	0.1186
2/18 19:20 - 2/19 06:40	0.0402	0.1112			